Skeletal Rearrangement in the Trinuclear *nido*-Ruthenacyclopentadiene Complexes: Theoretical and Experimental Studies

Akiko Inagaki,[†] Djamaladdin G. Musaev,*[,‡] Takemori Toshifumi,[†] Hiroharu Suzuki,*[,†] and Keiji Morokuma*[,‡]

Department of Applied Chemistry, Graduate School of Science and Engineering, Tokyo Institute of Technology and O-okayama Meguro-ku, Tokyo 152-8552, Japan, and Cherry L. Emerson Center for Scientific Computation and Department of Chemistry, Emory University, Atlanta, Georgia 30322

Received January 22, 2003

Thermolysis of trinuclear ruthenacyclopentadiene complexes $\{(C_5Me_5)Ru\}_2\{(C_5Me_5)RuCR^1CR^2CHCH\}(\mu\text{-}H)_3$ (**1**, $R^1 = Me$, $R^2 = H$; **3**, $R^1 = R^2 = Me$) affords the isomerization to $\{(C_5Me_5)Ru\}_2\{(C_5Me_5)RuCHCR^1CR^2CH\}(\mu\text{-}H)_3$ (**2**, $R^1 = Me$, $R^2 = H$; **4**, $R^1 = R^2 = Me$). Both products, **2** and **4**, were characterized by NMR spectroscopic data, while complex **2** was studied by X-ray crystallography. Kinetic studies show a small absolute value of activation entropy $\Delta S^{\ddagger} = 8.6(4)$ cal/mol/deg for **1** → **2**; −3.4(1) cal/mol/deg for **3** → **4**, indicating intramolecular character of these skeletal rearrangement reactions. Computational studies show that the mechanism I, involving the cyclobutadiene intermediate followed by C−C bond cleavage, is kinetically unfavorable for unsubstituted and mono- and dimethyl-substituted systems. The hydride-assisted mechanism II, involving (1) insertion of a C═C double bond into the Ru−H bond, (2) cleavage of a C−C bond to form the allylmethylene complex, (3) reductive coupling to reproduce the RuC_4 ring, and (4) C−H bond cleavage to give the final product, is found to be favorable. It proceeds with a rate-determining barrier (without zero-point correction) $\Delta E^{\ddagger}$ of 25−30 kcal/mol, which is in good agreement with the experimental $\Delta H^{\ddagger}$ values of 27.7 kcal/mol. For the isomerization of 2,3-dimethylruthenacyclopentadiene complex $\{(C_5Me_5)Ru\}_2\{(C_5Me_5)RuCMeCMeCHCH\}(\mu\text{-}H)_3$, it was shown that mechanism II.A leading to formation of 3,4-dimethyl-substituted product is more favored over mechanism II.B giving 2,5-dimethyl product.

1. Introduction

Metallacyclic compounds of the transition metals play an important role in the catalytic and stoichiometric reactions to produce natural products and novel organic molecules.[1] Their intermediacy in the oligomerization and metathesis of olefins,[2] as well as in the metal-mediated coupling reactions of alkynes,[2i,3] has been widely accepted. In the literature significant efforts have been made to understand the fragmentation and isomerization of metallacycles of mononuclear metallacyclopentadiene complexes.[4] However, only little is known on the fragmentation and isomerization of multinuclear metallacyclopentadiene complexes, which could be extremely useful in activation and catalytically transformation of inert molecules.[5] Understanding of these processes of metallacycles of multinuclear metallacyclopentadiene complexes could be instrumental to full utilization of inert molecules.

[†] Tokyo Institute of Technology.
[‡] Emory University.

(1) Chappell, S. D.; Cole-Hamilton, D. J. *Polyhedron* **1982**, *1*, 739.
(2) (a) Zuckerman, R. L.; Krska, S. W.; Bergman, R. G. *J. Am. Chem. Soc.* **2000**, *122*, 751. (b) Adlhart, C.; Hinderling, C.; Baumann, H.; Chen, P. *J. Am. Chem. Soc.* **2000**, *122*, 8204. (c) Aagard, O. M.; Meier, R. J.; Buda, F. *J. Am. Chem. Soc.* **1998**, *120*, 7174−7182. (d) Wang, S. S.; Vanderlende, D. D.; Abboud, K. A.; Boncella, J. M. *Organometallics* **1998**, *17*, 2628. (e) Dias, E. L.; Nguyen, S. T.; Grubbs, R. H. *J. Am. Chem. Soc.* **1997**, *119*, 3887. (f) Kress, J.; Osborn, J. A.; Greene, R. M. E.; Ivin, K. J.; Rooney, J. J. *J. Am. Chem. Soc.* **1987**, *109*, 899. (g) Katz, T. J.; Sivavec, T. M. *J. Am. Chem. Soc.* **1985**, *107*, 737. (h) Drâgutan, V.; Balaban, A. T.; Dimonie, M. *Olefin Metathesis and Ring-Opening Polymerization of Cyclo-Olefins*, 2nd rev. ed.; Wiley-Interscience: Chichester, U.K., 1985. (i) *Comprehensive Organometallic Chemistry*; Wilkinson, G., Stone, F. G. A., Abel, E. W., Eds.; Pergamon Press: Oxford, U.K., 1982; Vol. 8, pp 371−462. (j) Datta, S.; Fischer, M. B.; Wreford, S. S. *J. Organomet. Chem.* **1980**, *188*, 353. (k) McLain, S. J.; Sancho, J.; Schrock, R. R. *J. Am. Chem. Soc.* **1980**, *102*, 5610.
(3) (a) Rainer, D.; Bruce, E. E.; Gürtzgen, S.; Jalisatgi, S.; Matzger, A. J.; Radde, R. H.; Vollhardt, K. P. *J. Am. Chem. Soc.* **1998**, *120*, 8247. (b) Bönnemann, H.; Brijoux, W. *Applied Homogeneous Catalysis with Organometallic Compounds*; Cornils, B., Herrmann, W. A., Eds.; VCH: New York, 1996; Vol. 2. (c) Melikyan, G. G.; Nicholas, K. M. *Modern Acetylene Chemistry*; Stang, P. J., Diederich, F., Eds.; VCH: New York, 1995. (d) Trost, B. M. *Angew. Chem., Int. Ed. Engl.* **1995**, *34*, 259. (e) Grotjahn, D. B. *Comprehensive Organic Chemistry II*; Abel, E. W., Stone, F. G., Wilkinson G., Eds.; Pergamon Press: New York, 1994; Vol 12. (f) Parshall, G. W.; Ittel, S. D. *Homogeneous Catalysis*, 2nd ed.; Wiley: New York, 1992. (g) Schore, N. E. *Comprehensive Organic Synthesis*; Trost, B. M., Ed.; Pergamon Press: New York, 1990; Vol. 5. (h) Collman, J. P.; Hegedus, L. S.; Norton, J. R.; Finke, R. G. *Principles and Applications of Organotransition Metal Chemistry*; University Science Book: Mill Valley, CA, 1987. (i) Vollhardt, K. P. C. *Angew. Chem., Int. Ed. Engl.* **1984**, *23*, 539, and references therein. (j) Vollhardt, K. P. C. *Acc. Chem. Res.* **1977**, *10*, 1. (k) McAlister, D. M.; Bercaw, J. E.; Bergman, R. G. *J. Am. Chem. Soc.* **1977**, *99*, 1666.
(4) (a) Smith, D. P.; Stricker, J. R.; Gray, S. D.; Bruck, M. A.; Holmes, R. S.; Wigley, D. E. *Organometallics* **1992**, *11*, 1275. (b) Hill, J. E.; Fanwick, P. E.; Rothwell, I. P. *Organometallics* **1990**, *9*, 2211−2213. (c) Buchwald, S. L.; Nielsen, R. B. *J. Am. Chem. Soc.* **1989**, *111*, 2870−2874.

10.1021/om030046b CCC: $25.00
Publication on Web 03/20/2003

Recently, in an effort to activate C−H and C−C bonds of inert hydrocarbon molecules on multinuclear metallacyclopentadiene complexes, we have experimentally demonstrated that the C(sp^3)−C(sp^2) bond of cyclopentadiene is cleaved in the reaction with trinuclear ruthenium pentahydride cluster $\{(C_5Me_5)Ru\}_3(\mu\text{-}H)_2(\mu_3\text{-}H)_2$ under mild conditions (eq 1).[6] Surprisingly high reactivity of the hydrido cluster has been explained in terms of the cooperative action of adjacent metal centers with the substrate, where two metal centers act as "*coordination site*" and the other as "*activation site*". Numerous typical examples of such "*multimetallic activation*" have been demonstrated elsewhere.[7]

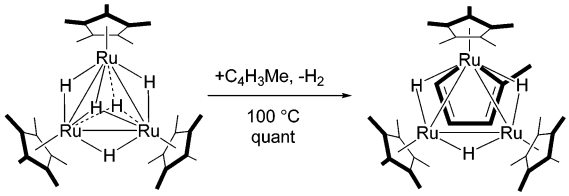

(1)

Also, we have discovered an unprecedented structural rearrangement of the ruthenacyclopentadiene, as shown in eqs 2 and 3 (see details of the experimental results in the next section),[8] in the thermolysis of these trinuclear compounds. The reaction of both **1** and **3**, $\{(C_5Me_5)Ru\}_2\{(C_5Me_5)RuCR^1CR^2CHCH\}(\mu\text{-}H)_3$ (**1**, $R^1 = Me$, $R^2 = H$; **3**, $R^1 = R^2 = Me$), proceeds at temperatures over 80 °C and results in the quantitative formation of seemingly isomerized products, 3-methylruthenacyclopentadiene complex (**2**) and 3,4-dimethylruthenacyclopentadiene complex (**4**), $\{(C_5Me_5)Ru\}_2\{(C_5Me_5)RuCHCR^1CR^2CH\}(\mu\text{-}H)_3$ (**2**, $R^1 = Me$, $R^2 = H$; **4**, $R^1 = R^2 = Me$), respectively. However, all attempts to detect the reaction intermediates, which is the most direct way for elucidating the reaction mechanism, were unsuccessful, and only the reactant and product of the reactions were observed by means of ^{1}H NMR spectroscopy.

To gain insight into the mechanism of these skeletal rearrangements, in the present paper we have carried out both experimental kinetic studies and density functional (DFT) studies of the reactions 2 and 3. Our data and their discussions are presented as follows. In section 2 we describe and discuss the results of experimental NMR kinetic studies, while in section 3 the method and results of computational studies are presented and discussed. In section 4 we draw a few conclusions from our studies.

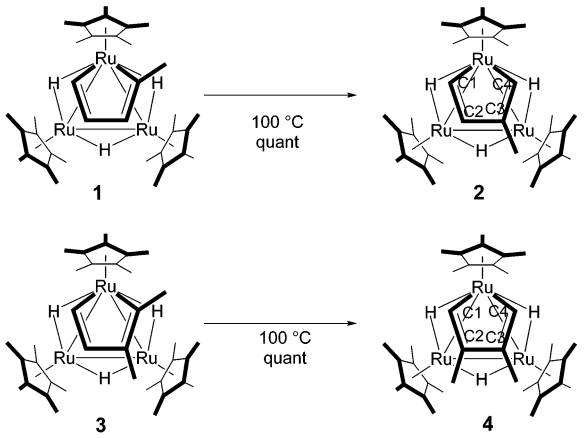

(2)

(3)

2. Results and Discussion of Experimental NMR Kinetic Studies

Experimental data show that heating a solution of 2-methylruthenacyclopentadiene complex **1** in benzene-d_6 at 100 °C for 36 h results in the quantitative formation of 3-methylruthenacyclopentadiene complex $\{(C_5Me_5)Ru\}_2\{(C_5Me_5)RuCHCMeCHCH\}(\mu\text{-}H)_3$ (**2**), in which methyl substituent has seemingly moved from the fourth to the third position (eq 2). The resulting complex **3** has been characterized by ^{1}H and ^{13}C NMR and IR spectroscopy. Resonance signals of protons attached to C1 and C4 (eq 2) are observed at δ 7.10 (J = 2.4 Hz) and 7.05 (J = 4.5 Hz) as doublets, respectively, and the proton attached to C2 is observed at δ 3.69 as doublets of a doublet. In the ^{13}C NMR spectrum, resonances of C1 and C4 are observed at relatively low field, at δ 167.9 and 162.0, due to the carbene character of the carbons, while signals for C2 and C3 appear at δ 68.2 and 76.8, respectively. The X-ray diffraction study confirmed the proposed structure of **2**. The ORTEP drawing of **2** is displayed in Figure 1 along with some of the relevant bond distances and angles.

Thermolysis of 2,3-dimethylruthenacyclopentadiene complex $\{(C_5Me_5)Ru\}_2\{(C_5Me_5)RuCMeCMeCHCH\}(\mu\text{-}H)_3$ (**3**) in toluene at 110 °C for 18 h afforded a new product, which was isolated as a purple-brown crystalline solid in a 66.5% yield and assigned as a 3,4-dimethylruthenacyclopentadiene complex $\{(C_5Me_5)Ru\}_2\{(C_5Me_5)RuCHCMeCMeCH\}(\mu\text{-}H)_3$ (**4**) based on the observation of equivalent sets of proton resonances at δ 7.13 (2H, C1-*H*, C4-*H*) and 1.84 (6H, $-CH_3 \times 2$) for the ruthenacyclopentadiene moiety (eq 3).[9] In the ^{13}C NMR spectrum, signals for C1 and C4, C2 and C3 (eq 3), and two of the methyl groups on the ruthenacycle are observed to be equivalent at δ 168.5 (d, J_{CH} = 149.3 Hz), 77.8 (s), and 25.6 (q, J_{CH} = 124.1 Hz), respectively. Despite careful monitoring of the reaction by means of ^{1}H NMR spectroscopy, none of the resonance attributable to intermediates was observed during the reaction.

It is noteworthy that in the literature several examples of skeletal rearrangement of mononuclear metallacyclopentenes and metallacyclopentadienes have

(5) For examples of trinuclear metallacyclopentadiene complexes, see: (a) Koridze, A. A.; Sheloumov, A. M.; Petrovskii, P. V., Tok, O. L. *Russ. Chem. Bull.* **1999**, *48*, 1015. (b) Koridze, A. A.; Sheloumov, A. M.; Dolgushin, F. M.; Yanovsky, A. I.; Struchkov, Y. T.; Petrovskii, P. V. *Russ. Chem. Bull.* **1996**, *45*, 702. (c) Nizamov, I. S.; Garifzyanova, G. G.; Batyeva, E. S. *Russ. Chem. Bull.* **1994**, *43*, 718. (d) Koridze, A. A.; Astakhova, N. M.; Dolgushin, F. M.; Yanovsky, A. I.; Struchkov, Y. T.; Petrovsky, P. V. *Organometallics* **1995**, *14*, 2167.

(6) (a) Suzuki, H.; Takaya, Y.; Takemori, T. *J. Am. Chem. Soc.* **1994**, *116*, 10779. (b) Takemori, T.; Takaya, Y.; Inagaki, A.; Tanaka, M.; Suzuki, H. Unpublished results.

(7) (a) Suzuki, H. *Eur. J. Inorg. Chem.* **2002**, *5*, 1009−1023. (b) Takao, T.; Yoshida, S.; Suzuki, H. *Chem. Lett.* **2001**, *11*, 1100−1101. (c) Okamura, R.; Tada, K.; Matsubara, K.; Oshima, M.; Suzuki, H. *Organometallics* **2001**, *20*, 4772−4774. (d) Takao, T.; Amako, M.; Suzuki, H. *Organometallics* **2001**, *20*, 3406−3422. (e) Ohki, Y.; Kojima, T.; Oshima, M.; Suzuki, H. *Organometallics* **2001**, *20*, 2654−2656. (f) Inagaki, A.; Takemori, T.; Tanaka, M.; Suzuki, H. *Angew. Chem., Int. Ed.* **2000**, *39*, 404−406. (g) Matsubara, K.; Inagaki, A.; Tanaka, M.; Suzuki, H. *J. Am. Chem. Soc.* **1998**, *120*, 1108−1109. (h) Inagaki, A.; Takaya, Y.; Takemori, T.; Suzuki, H. *J. Am. Chem. Soc.* **1997**, *119*, 625−626.

(8) Inagaki, A.; Takemori, T.; Suzuki, H. Unpublished results.

(9) A preliminary X-ray diffraction study for **4** showed the 3,4-dimethylruthenacyclopentadiene structure.

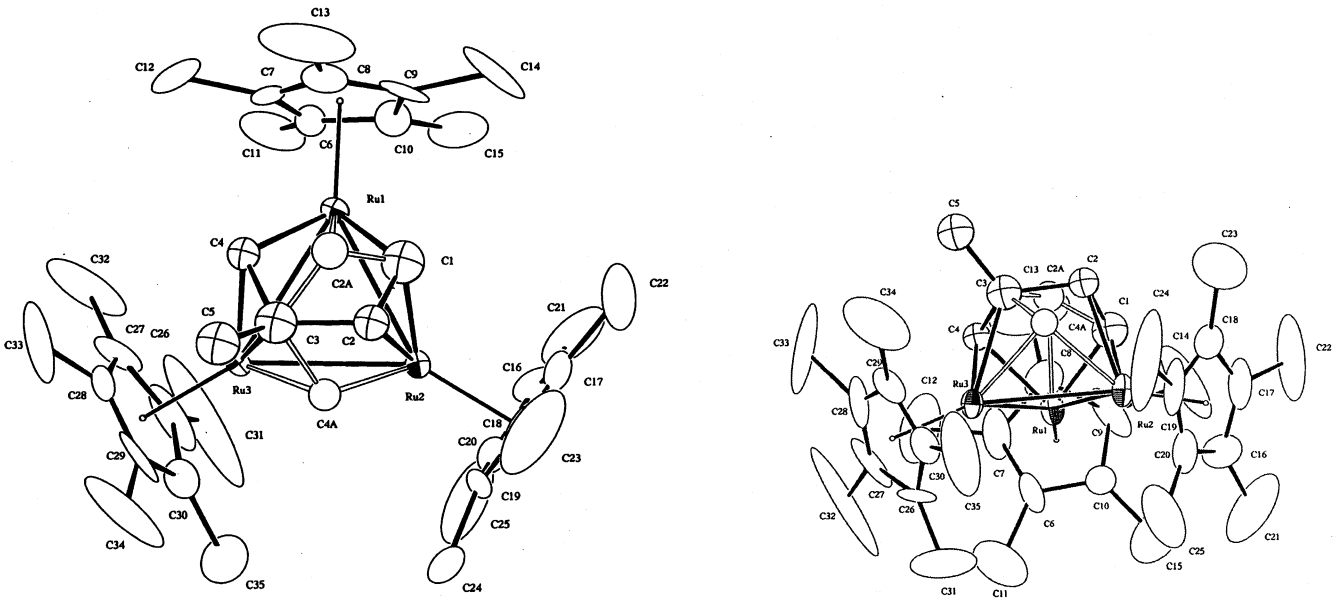

Figure 1. X-ray structure of $\{(C_5Me_5)Ru\}_2\{(C_5Me_5)RuCHCMeCHCH\}(\mu\text{-}H)_3$ (**2**), with thermal ellipsoids at the 30% probability level. Selected bond lengths (Å) and angles (deg) are as follows: Ru(1)−Ru(2) 2.830(2), Ru(1)−Ru(3) 2.881(2), Ru(2)−Ru(3) 2.879(2), Ru(1)−C1 2.04(2), Ru(1)−C(4) 2.13(4), Ru(2)−C(1) 2.02(2), Ru(2)−C(2) 2.29(4), Ru(3)−C(3) 2.30(2), Ru(3)−C(4) 2.17(3); Ru(1)−Ru(2)−Ru(3) 60.61(5), Ru(2)−Ru(3)−Ru(1) 58.85(5), Ru(2)−Ru(1)−Ru(3) 60.54(5), Ru(1)−C(1)−C(2) 124(2), C(1)−C(2)−C(3) 105(2), C(3)−C(4)−Ru(1) 112(2).

Scheme 1. Schematic Presentation of the Fragmentation-Recombination Mechanism for the Skeletal Rearrangement in the Trinuclear Ruthenacyclopentadiene Complexes[a]

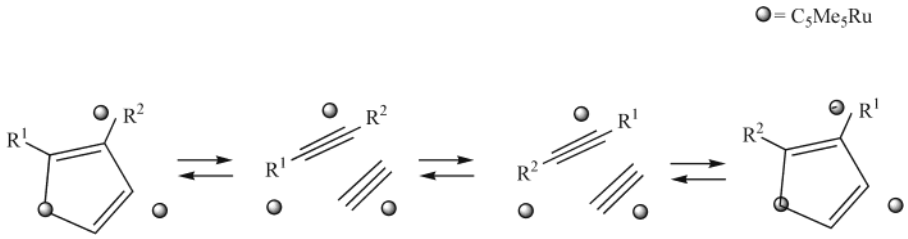

[a] Cyclopentadienyl and hydride ligands were omitted for simplicity.

been reported,[10] and this rearrangement is best interpreted by the mechanism involving a fragmentation of the metallacycle into the metal center and two alkenes/alkyne or alkyne fragments (Scheme 1). However, the similar "fragmentation-recombination" explanation for the skeletal rearrangement of complex **3** to **4** in the multinuclear ruthenacyclopentadiene is not feasible, since the thermolysis of dimethylruthenacyclopentadiene complex **3** with methyl groups on the α,β position results in the formation of β,β′-dimethyl products **4**.

In an effort to gain insight into the mechanism, we have performed NMR kinetic studies of the skeletal rearrangement. The experimental procedure of the present NMR kinetic studies is summarized in the Supporting Information. Temperature dependence of the first-order rate constant (k_1) was used in deriving Arrhenius activation parameters, $\Delta H^{\ddagger}$and $\Delta S^{\ddagger}$. The activation parameters deduced from the first-order rate constants are found to be $\Delta H^{\ddagger} = 26.2(22)$ kcal/mol, $\Delta S^{\ddagger} = 8.6(4)$ cal/mol/deg for eq 2, $\Delta H^{\ddagger} = 27.7(17)$ kcal/mol, $\Delta S^{\ddagger} = -3.4(1)$ cal/mol/deg for eq 3. The relatively small absolute value of the activation entropy for these reactions shows that the both reactions proceed *intramolecularly*. This conclusion is also supported by the fact that heating a 2-methylruthenacyclopentadiene complex **1** in toluene under atmospheric acetylene at 100 °C for 14 h results in the quantitative formation of 3-methylruthenacyclopentadiene complex **2**, while none of the nonsubstituted ruthenacyclopentadiene complexes formed.

(10) Takahashi, T. *J. Synth. Org. Chem.* **1990**, *48*, 476.

3. Computational Studies of Isomerization Mechanisms

A. Computational Models and Method. In our computational studies we adopt the unsubstituted ruthenacyclopentadiene complexes and examine two different reaction mechanisms, I and II (see Scheme 2), both of which are consistent with available experimental data and are *intramolecular* in nature. The first of them, mechanism I, involves the cyclobutadiene species and consists of two steps: (1) reductive coupling of ruthenacyclopentadiene to form cyclobutadiene unit, step **5** → **6**, and (2) C−C bond cleavage of the cyclobutadiene ring to give the product, step **6** → **5**. The notable feature of this mechanism is the formation of a trinuclear cyclobutadiene complex, which has never been isolated or reported until today. An alternative mechanism, mechanism II, is a multistep pathway and involves (1) insertion of a C═C double bond into the Ru−H bond,

Scheme 2. Two Possible Reaction Mechanisms for Intramolecular Skeletal Rearrangement in Trinuclear Ruthenacyclopentadiene Complexes

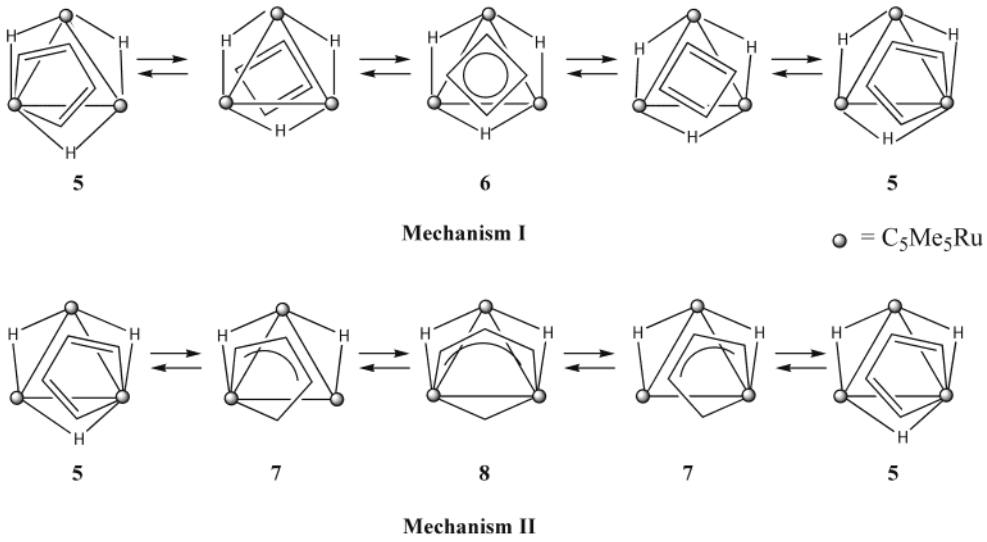

step **5** → **7**, (2) cleavage of a C−C bond to form the allylmethylene complex, step **7** → **8**, (3) reductive coupling to reproduce the RuC_4 ring, step **8** → **7**, and (4) C−H bond cleavage to give the final product, step **7** → **5**.

Here we have adopted the following strategy. At first, we have studied the proposed mechanisms of the reaction for the model complex, where the methyl groups of the experimentally used cyclopentadiene rings were replaced by hydrogen atoms. At the next stage, we elucidate the substituent effect by performing single-point energy calculations for experimentally used systems at the geometries obtained for the model system. Model structures for the single-point energy calculation are constructed by replacing two hydrogen atoms on the ruthenacyclopentadiene ring by two methyl groups with known C(sp^3)−H bond lengths and angles.

All calculations were performed using the hybrid B3LYP density functional method, which uses Becke's three-parameter nonlocal exchange functional[11] mixed with the exact (Hartree−Fock) exchange functional and Lee−Yang−Parr's nonlocal correlation functional.[12] Geometries of all the reactants, intermediates, transition states (TSs), and products were optimized with the analytical gradient method. For geometry optimization we used the lanl2dz basis set[13] for all atoms except for the C and H atoms of cyclopentadienyl ligands, for which we used the split-valence 3-21G basis set (this combination of the basis sets will be called BS1). The starting geometries for optimization of the reactant and the product, which possess trinuclear ruthenacyclopentadiene skeleton, are taken from the X-ray crystallographic data of the *nido*-3,4-dimethylruthenacyclopentadiene complex $\{(C_5Me_5)Ru\}_2\{(C_5Me_5)RuCHCMeCMeCH\}(\mu\text{-}H)_3$.[14] To confirm the nature of the calculated TS, *pseudo*-IRC (intrinsic reaction coordinate) calculations were carried out in the following manner. The geometry of the transition state was at first shifted, toward both the reactant and the product side, respectively, based on the eigenvector of the imaginary frequency of the approximate Hessian, and released for equilibrium optimization. In this manner, each transition state was connected to the reactant and the product of the respective step. To obtain more reliable energetics, single-point energy calculations at the B3LYP level using the Stuttgart/Dresden effective core potential (ECP)[15] and associated basis sets for Ru, 6-311G(d,p) for hydrides and (ruthena)cyclopentadiene,[16] and 6-31+G-(d) basis sets for Cp ligands[17] (below called BS2) have been performed at the B3LYP/BS1 optimized geometries. Previously,[18] it was demonstrated that the B3LYP method with double-ζ quality basis sets, such as lanl2dz, for geometry optimization, and triple-ζ quality basis sets, such as SDD, for relative energy calculations provide reasonable agreement with available experimental data and high-level methods, while it often underestimates the barriers by a few kcal/mol.[19] In this paper we mostly discuss the calculated chemical trends and relative energies, and we believe that the underestimation of the barriers by a few kcal/mol at the

(11) (a) Becke, A. D. *Phys. Rev. A* **1988**, *38*, 3098. (b) Becke, A. D. *J. Chem. Phys.* **1993**, *98*, 5648.
(12) Lee, C.; Yang, W.; Parr, R. G. *Phys. Rev. B* **1988**, *37*, 785.
(13) (a) Dunning, T. H., Jr.; Hay, P. J. in *Modern Theoretical Chemistry*; Schaefer, H. F., III, Ed.; Plenum: New York, 1976; pp 1−28. (b) Hay, P. J.; Wadt, W. R. *J. Chem. Phys.* **1985**, *82*, 270. (c) Wadt, W. R.; Hay, P. J. *J. Chem. Phys.* **1985**, *82*, 284. (d) Hay, P. J.; Wadt, W. R. *J. Chem. Phys.* **1985**, *82*, 299.
(14) Inagaki, A.; Suzuki, H. Unpublished results.
(15) Andrae, D.; Haeussermann, U.; Dolg, M.; Stoll, H.; Preuss, H. *Theor. Chim. Acta* **1990**, *77*, 123.
(16) (a) McLean, A. D.; Chandler, G. S. *J. Chem. Phys.* **1980**, *72*, 5639. (b) Krishnan, R.; Binkley, J. S.; Seeger, R.; Pople, J. A. *J. Chem. Phys.* **1980**, *72*, 650.
(17) See ref 21, and references therein.
(18) (a) Cui, Q.; Musaev, D. G.; Svensson, M.; Sieber, S.; Morokuma, K. *J. Am. Chem. Soc.* **1995**, 117, 12366. (b) Musaev, D. G.; Morokuma, K. *J. Phys. Chem.* **1996**, *100*, 6509. (c) Erikson, L. A.; Pettersson, L. G. M.; Siegbahn, P. E. M.; Wahlgren, U. *J. Chem. Phys.* **1995**, *102*, 872. (d) Ricca, A.; Bauschlicher, C. W., Jr. *J. Phys. Chem.* **1994**, *98*, 12899. (e) Heinemann, C.; Hertwig, R. H.; Wesendrup, R.; Koch, W.; Schwarz, H. *J. Am. Chem. Soc.* **1995**, *117*, 495. (f) Hertwig, R. H.; Hrusak, J.; Schroder, D.; Koch, W.; Schwarz, H. *Chem. Phys. Lett.* **1995**, *236*, 194. (g) Schroder, D.; Hrusak, J.; Hertwig, R. H.; Koch, W.; Schwerdtfeger, P.; Schwarz, H. *Organometallics* **1995**, *14*, 312. (i) Fiedler, A.; Schroder, D.; Shaik, S.; Schwarz, H. *J. Am. Chem. Soc.* **1994**, *116*, 10734. (h) Fan, L.; Ziegler, T. *J. Chem. Phys.* **1991**, *95*, 7401. (j) Berces, A.; Ziegler, T.; Fan, L. *J. Phys. Chem.* **1994**, *98*, 1584. (k) Lyne, P. D.; Mingos, D. M. P.; Ziegler, T.; Downs, A. J. *Inorg. Chem.* **1993**, *32*, 4785. (l) Li, J.; Schreckenbach, G.; Ziegler, T. *J. Am. Chem. Soc.* **1995**, *117*, 486.
(19) (a) Lynch, B. J.; Fast, P. L.; Harris, M.; Truhlar, D. G. *J. Phys. Chem. A* **2000**, *104*, 4811. (b) Bach, R. D.; Glukhovtsev, M. N.; Canepa, C. *J. Am. Chem. Soc.* **1998**, *120*, 775.

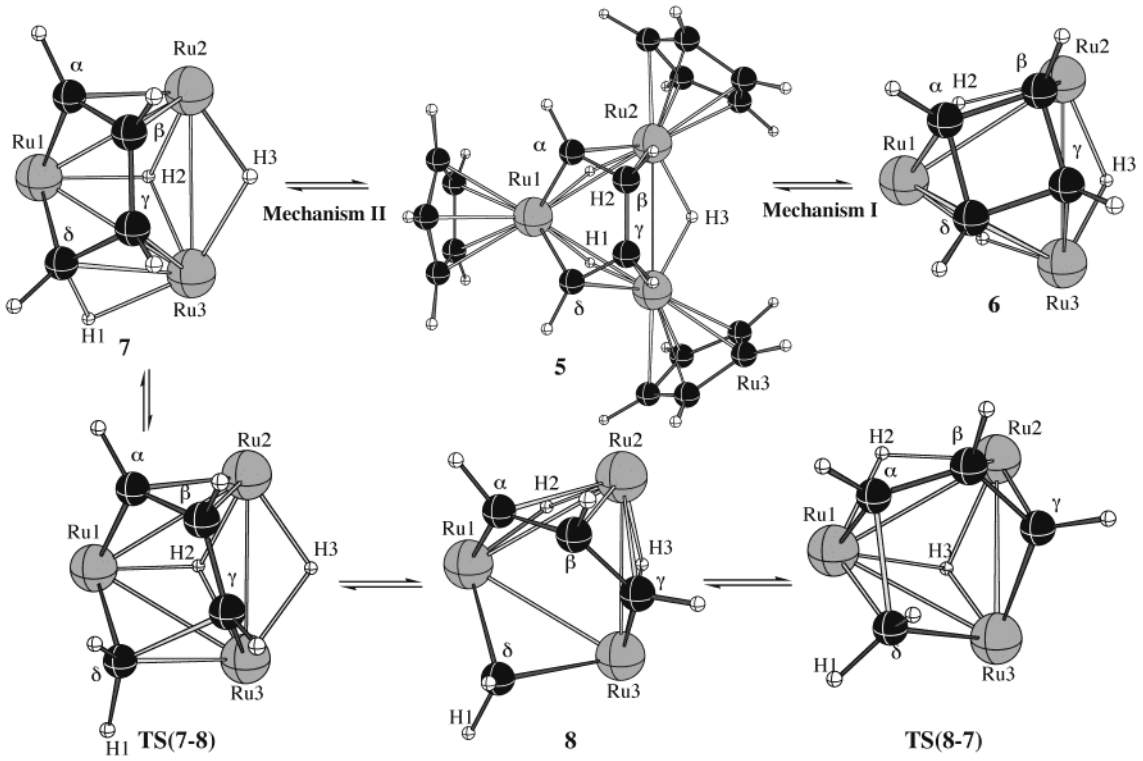

Figure 2. Calculated intermediates and transition states of the mechanisms I and II of skeletal rearrangement of the complex $\{(C_5H_5)Ru\}_2\{(C_5H_5)RuC_4H_4\}(\mu\text{-}H)_3$ (**5**). All the calculated geometrical parameters of these structures are presented in the Supporting Information, while the most important ones are given in Table 1. For simplicity the Cp ligands were omitted, except for **5**.

B3LYP/SDD level will not affect our conclusions. Considering the size of the system, no Hessian matrix and hence no zero-point energy were calculated. All calculations were carried out with the Gaussian 98 program.[20]

One should note that the geometries of the reactants, intermediates, transition states, and products of the reaction mechanisms I and II were fully optimized without any symmetry constraint, except for structures **5**, **6**, and **8**. Since these structures possess pseudo-C_s symmetry, local C_s symmetry has been assumed for these structures. However, when C_s symmetry is assumed, there exists two isomers, **a** and **b**, according to the orientation of the Cp ligands with respect to the C_s symmetry plane, which should be distinguished; in isomer **a** the carbon atom located on the symmetry plane is on the same side of the Ru_3 plane as the other similar C atoms from the other two Cp rings, while in isomer **b** they are located on different sides of the Ru_3 plane. The rotation of the Cp rings is expected to be very easy, and paths from isomers **a** and **b** need not be discussed separately. Thus in the following we always assume isomer **a** for all the species.

B. Results and Discussion for Cyclobutadiene Mechanism I. Unsubstituted Ruthenacyclopentadienyl Model Complex. This reaction pathway starts with complex **5**, $\{(C_5H_5)Ru\}_2\{(C_5H_5)RuC_4H_4\}(\mu\text{-}H)_3$, the optimized structure of which is shown in Figure 2. In Table 1, we compare the calculated important geometrical parameters of unsubstituted compound **5** with those of the corresponding C_5Me_5 compound, $\{(C_5Me_5)Ru\}_2\{(C_5Me_5)RuC(CH_3CHCHCH\}(\mu\text{-}H)_3$, **2**, determined by the X-ray study in Figure 1, while full Cartesian coordinates of complex **5** are given in the Supporting Information.

As seen in Table 1, the calculated Ru−Ru bond lengths of 2.859, 3.009, and 2.859 Å are in good agreement with their experimental values of 2.860(2), 2.916(2), and 2.866(2) Å. However, the average value of the calculated $Ru-C^{Cp-ring}$ distances is 0.10 Å longer than the corresponding experimental data. This large difference in the calculated and experimental average $Ru-C^{Cp-ring}$ distances could be a result of replacement of Cp* by Cp in our calculations; the electron-donative Me groups are likely to make the Cp ring more strongly bound to the metal. Overall, the ruthenacyclopentadiene unit is reproduced well by this level of calculation with the Cp model complex. Indeed, the calculated Ru−C, C−C, and C−H bond distances of the ruthenacyclopentadiene unit only slightly (±3.0%, which does not include the $Ru-C^{Cp-ring}$ bond lengths) differ from their corresponding experimental values. In other words, these results indicate that the intramolecular skeletal rearrangement of Cp*Ru complexes can be correctly described using the corresponding CpRu model complexes.

In the first step of mechanism I the reductive C−C coupling in ruthenacyclopentadiene occurs to form a cyclobutadiene unit. The resulting cyclobutadiene com-

(20) Frisch, M. J.; Trucks, G. W.; Schlegel, H. B.; Scuseria, G. E.; Robb, M. A.; Cheeseman, J. R.; Zakrzewski, V. G.; Montgomery, J. A., Jr.; Stratmann, R. E.; Burant, J. C.; Dapprich, S.; Millam, J. M.; Daniels, A. D.; Kudin, K. N.; Strain, M. C.; Farkas, O.; Tomasi, J.; Barone, V.; Cossi, M.; Cammi, R.; Mennucci, B.; Pomelli, C.; Adamo, C.; Clifford, S.; Ochterski, J.; Petersson, G. A.; Ayala, P. Y.; Cui, Q.; Morokuma, K.; Malick, D. K.; Rabuck, A. D.; Raghavachari, K.; Foresman, J. B.; Cioslowski, J.; Ortiz, J. V.; Stefanov, B. B.; Liu, G.; Liashenko, A.; Piskorz, P.; Komaromi, I.; Gomperts, R.; Martin, R. L.; Fox, D. J.; Keith, T.; Al-Laham, M. A.; Peng, C. Y.; Nanayakkara, A.; Gonzalez, C.; Challacombe, M.; Gill, P. M. W.; Johnson, B. G.; Chen, W.; Wong, M. W.; Andres, J. L.; Head-Gordon, M.; Replogle, E. S.; Pople, J. A. *Gaussian 98*; Gaussian, Inc.: Pittsburgh, PA, 1998.

Table 1. Calculated Important Geometrical Parameters of the Reactant, Intermediates, and Transition States Corresponding to the Skeletal Rearrangement of the Complex $\{(C_5H_5)Ru\}_2\{(C_5H_5)RuC_4H_4\}(\mu\text{-}H)_3$, 5, and the X-ray Experimental Value for $\{(C_5Me_5)Ru\}_2\{(C_5R_5)RuCMeCHCHCH\}(\mu\text{-}H)_3$, 2[a]

parameter	**5**/**2** (exptl)	**6**	**7**	**TS(7−8)**	**8**	**TS(8−7)**
Ru1−Ru2	2.859/ 2.860(2)	2.968	2.811	2.824	2.842	2.868
Ru1−Ru3	2.859/ 2.866(2)	2.968	2.916	2.799	2.829	2.799
Ru2−Ru3	3.009/ 2.916(2)	2.826	2.889	2.868	2.842	2.824
av (Ru−Ru)	2.909/ 2.881(2)					
Ru1−C^{α}	2.066/ 2.11(2)	2.076	2.026	2.010	1.985	2.000
Ru1−C^{δ}	2.066/−	2.065	2.062	2.067	2.191	
Ru2−C^{α}	2.089/ 2.14(2)		2.119	2.127	2.294	2.865
Ru2−C^{β}	2.257/ 2.28(2)	2.106	2.242	2.285	2.264	2.285
Ru2−C^{γ}		2.999	2.865	2.294	2.127	
Ru3−C^{γ}	2.257/ 2.20(2)	2.245	2.190	2.000	1.985	2.010
Ru3−C^{δ}	2.089/ 2.08(2)	2.106	2.266	2.191	2.067	2.062
av (Ru−$C^{Cp-ring}$)	2.312/ 2.21(2)					
Ru3−H1	1.705		1.778			
C^{d}−H1			1.234	1.101	1.100	1.101
C^{α}−C^{β}	1.438/ 1.42(3)	1.516	1.441	1.453	1.437	1.452
C^{β}−C^{γ}	1.471/ 1.41(3)	1.547	1.481	1.452	1.437	1.453
C^{γ}−C^{δ}	1.438/ 1.45(2)	1.547	1.498	1.956	2.719	2.640
C^{α}−C^{δ}		1.516	2.607	2.640	2.719	1.956

[a] For definitions of the presented parameters, see Figure 2. All distances are in Å.

plex **6** was optimized under the C_s symmetry constraint. The obtained structure (excluding the cyclopentadienyl ligands) and important geometrical parameters are shown in Figure 2 and Table 1. As seen from this figure and Table 1, there are two different C−C bond distances in the cyclobutadiene unit, 1.516 and 1.547 Å, which are similar to the bond lengths of typical C−C single bonds (1.53 Å). The two angles of the C4 ring (not shown in Table 1) are 88.4° and 92.4°, respectively, showing a slight distortion from a true square. The formed C_4H_4 unit is coordinated to the Ru_3 fragment in a staggered manner with two carbon atoms on a C_s symmetry plane. The frequency calculations give an imaginary frequency of 192.9i cm^{-1} with a″ symmetry, indicating that the calculated cyclobutadiene structure is not a minimum but a transition state. The pseudo-IRC calculations have shown that this is the transition state directly connecting the reactant **5** and the equivalent product **5**. Calculations of the low-lying singlet and triplet states of this transition state indicate the closed shell singlet state to be the ground state.

In Figure 3A we have presented the potential energy diagram of the mechanism I. As you can see from this figure, the barrier height (without zero-point energy correction) connecting reactant **5** with product **5** at the transition state **6** is about 48−49 kcal/mol. Single-point energy calculations performed using the large basis sets (BS2, given in parentheses) increase the calculated barrier height by ca. 7 kcal/mol to 55.2 kcal/mol. These values are nearly twice as large as the above-reported experimental values, $\Delta H^{\ddagger} = 26.2(22)$ and 27.7(17) kcal/mol, for the monomethyl- and dimethyl-substituted systems, respectively.

Substituted Ruthenacyclopentadienyl Complexes. One of the reasons for such a large discrepancy between the calculated and experimental values of the energetic barrier for skeletal rearrangement in the triruthenium complex could be the use of a model complex in our calculations, which does not include any methyl substituents. Therefore, we have recalculated the skeletal rearrangement barrier for the mono- and dimethyl-substituted systems: $\{(C_5H_5)Ru\}_2\{(C_5H_5)$-$RuCMeCHCHCH\}(\mu\text{-}H)_3$ (**5-α-Me**) and $\{(C_5H_5)Ru\}_2$-$\{(C_5H_5)RuCMeCMeCHCH\}(\mu\text{-}H)_3$ (**5-αβ-diMe**).

Full optimization of the geometries of **5-α-Me**, **5-β-Me**, **7-α-Me**, **7-γ-Me**, and **8-α-Me** complexes (see Supporting Information) and comparing the obtained geometrical parameters with those for the unsubstituted model complexes **5**, **7**, and **8**, respectively, show that the substitution of one of the hydrogen ligands in the model complexes by a methyl group has only an insignificant effect on the geometries. This was also confirmed by calculating the total energies of these monomethyl-substituted systems by using optimized geometries and those from the corresponding unsubstituted model complexes: the former energies are found to be only ca. 1.5 kcal/mol lower than the latter. Therefore, below, in the calculations of the mono- and dimethyl-substituted systems we used only the optimized structures of the unsubstituted model complexes and transition states. It is noteworthy that when methyl substituents are taken into account in the model complexes, the potential energy surface of the skeletal rearrangement becomes asymmetric with respect to the transition state. Now, the transition state **6-Me** connects reactant **5-α-Me** (methyl group is located on C^{α}) with product **5-β-Me** (methyl is located on C^{β}). Meanwhile, for the dimethyl-substituted system, the transition state **6-diMe** connects reactant **5-αβ-diMe** with **5-ββ′-diMe**.

In Figure 3B,C we have presented the calculated energetics for monomethyl- and dimethyl-substituted systems, respectively. As seen from these figures the reactions for monomethyl- and dimethyl-substituted systems are exothermic by ca. 1.0−1.8 kcal/mol, which is consistent with the experiment showing the 100% conversion under thermal conditions. However, the calculated barriers for the **5-Me** and **5-diMe** complexes still are large, ca. 47−49 kcal/mol, compared to the experimentally reported value of $\Delta H^{\ddagger} = 26.2(22)$ kcal/mol and $\Delta H^{\ddagger} = 27.7(17)$ kcal/mol, respectively.

Thus, the above presented results show that neither the methyl-substituted models nor the larger basis sets significantly reduced the discrepancy between calculated and experimental results. On the basis of these results we conclude that mechanism I is not the true mechanism for the thermal skeletal rearrangement process in the trinuclear ruthenacyclopentadiene complex.

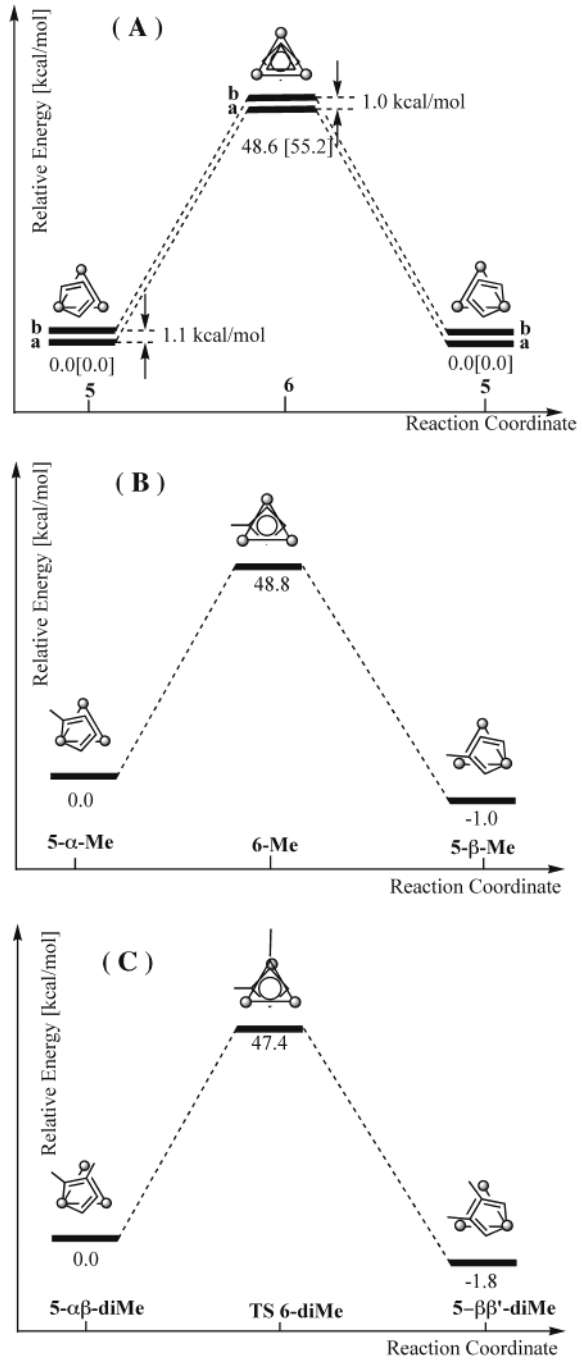

Figure 3. Potential energy profile of mechanism I for the intramolecular skeletal rearrangement in (A) unsubstituted model complex **5**, (B) **5-α-Me**, and (C) **5-αβ-diMe**. Numbers in square brackets were calculated at the BS2 basis set.

C. Results and Discussion for Hydride-Assisted Mechanism II. Unsubstituted Ruthenacyclopentadienyl Complexes. As we can see from Scheme 2, this reaction pathway also starts from the reactant **5**, but is followed by the formation of two additional intermediates, **7** and **8**. The search for intermediate **7** has been carried out without any symmetry constraint, while the geometry of intermediate **8** was calculated under the C_s symmetry constraint. The obtained structures (excluding the cyclopentadienyl ligands) of intermediates **7** and **8** were presented in Figure 2, while their important geometrical parameters are given in Table 1.

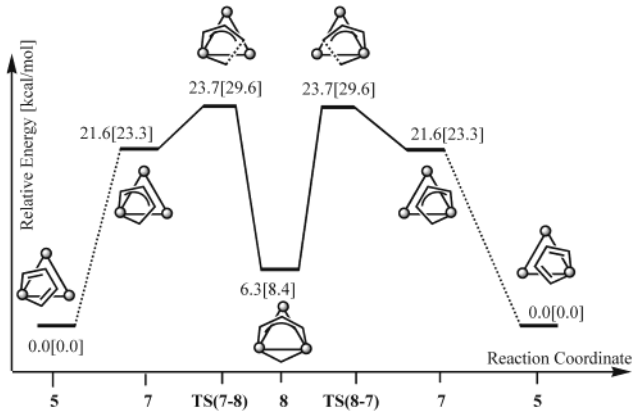

Figure 4. Potential energy profile of mechanism II for the intramolecular skeletal rearrangement in unsubstituted model complex **5**. Numbers in square brackets were calculated at the BS2 basis set.

As seen from Figure 2 and Table 1, the structural differences between the reactant **5** and intermediate **7** are mainly in the position of the bridging hydride ligands. In **7**, one of the hydride ligands (H2) moved from the μ_2- to the μ_3-position. Another hydride ligand (H^1) moved from the bridging position between two Ru centers in **5** to the bridging position between a ruthenium and δ-carbon atoms of the ruthenacyclopentadiene ring in **7**. The calculated important bond distances of complex **7** are Ru3−C^δ = 2.266 Å, Ru3−H1 = 1.778 Å, and C^δ−H1 = 1.234 Å. As a result of the formation of the C^δ−H1 bond, the C^δ−C^γ bond length has slightly (0.06 Å) lengthened to 1.498 Å. The C^δ−Ru3 bond distance was also lengthened to 2.266 Å, which was about 0.18 Å longer than the corresponding bond length of the reactant (C^δ−Ru3, 2.089 Å), complex **5**.

Unfortunately, we were unable to locate the transition state connecting structures **5** and **7**. All our potential energy scanning calculations indicate the existence of a barrier between **5** and **7**, with a very small barrier height from **7**. For example, our scanning of the potential energy surface by varying three independent parameters (C^δ−H1 bond distance, position of the centroid of the Cp ligand coordinated to Ru1, and the dihedral angle of H2 from the μ_2- to μ_3-hydride position) gives only a very small energy barrier, calculated from **7**, which disappeared during the transition state search. Since the **5** → **7** transformation is highly (21−23 kcal/mol) endothermic, it is expected that the transition state separating **5** and **7** is located closer to the product **7**. Furthermore, since the energy difference between the scanned "transition state" and **7** is small, one may take the energy difference between **5** and **7** as an approximate barrier height for **5** to **7** rearrangement.

As seen from Figure 4, where we have presented the potential energy surface of the reaction based on mechanism II, structure **7** lies several kcal/mol lower than transition state **TS(7−8)**, separating it from the most favorable product **8**. The intermediate **8** has a μ_3-allylmethylene type of structure with C−C bond distances of the allyl ligand of 1.437 Å and a bridging methylene ligand with a Ru3−C^δ bond distance of 2.067 Å, which is within a typical Ru−C σ bond length. The methylene fragment is located on the same side of the allyl (C3) fragment, but C^γ−C^δ bond cleavage is clearly shown by the calculated bond distance of 2.719 Å.

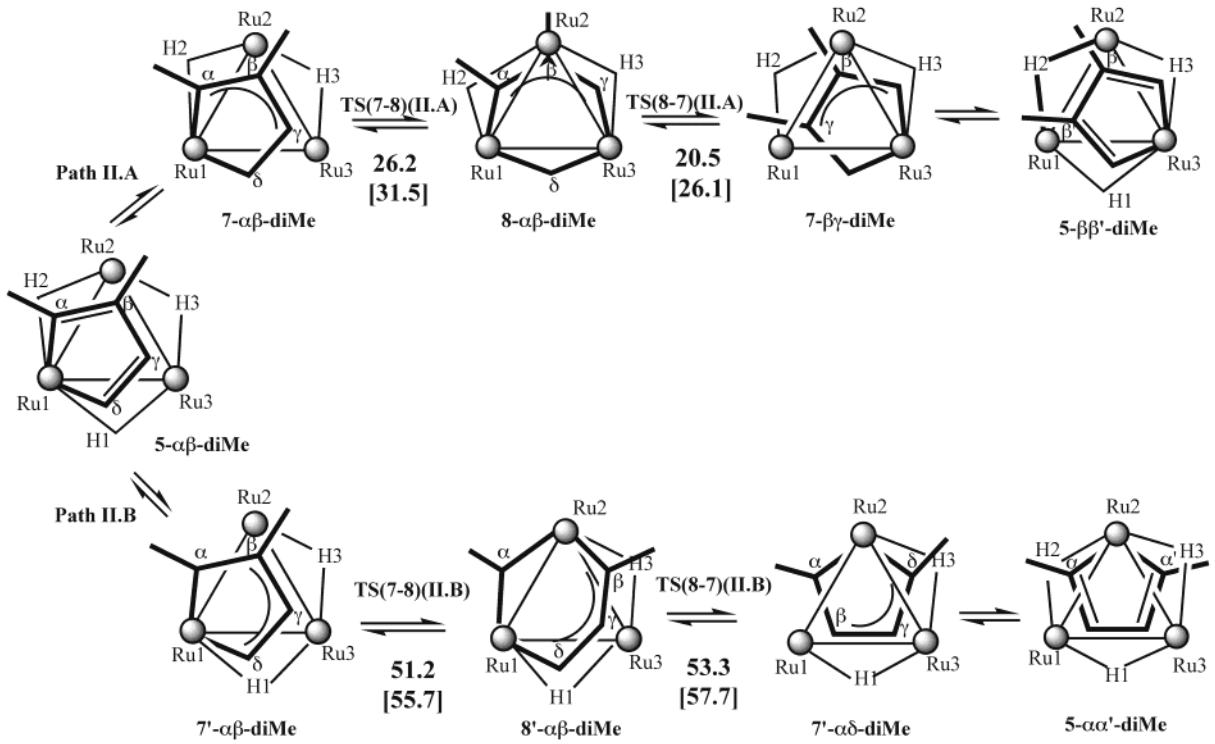

Figure 5. Two possible reaction pathways, path II.A and path II.B, for the intramolecular skeletal rearrangement in **5-α*β*-diMe** corresponding to the initial hydride transfer process to C^{α} and C^{β}, respectively. Numbers in square brackets were calculated at the BS2 basis set.

The transition state structure of **TS(7−8)** connecting intermediates **7** and **8** was successfully located and is presented in Figure 2. As seen from this figure and Table 1, the $C^{\gamma}-C^{\delta}$ bond length is lengthened to 1.956 Å, indicating **TS(7−8)** is the $C^{\gamma}-C^{\delta}$ bond cleavage transition state. Bond distances for $C^{\alpha}-C^{\beta}$ and $C^{\beta}-C^{\gamma}$ are calculated to be 1.45 Å. These bond lengths are 0.03 and 0.04 Å shorter than those in **5** and **7**, respectively. Frequency calculations for the optimized transition state gave only one imaginary frequency, 304.6i cm^{-1}, corresponding to the $C^{\gamma}-C^{\delta}$ bond cleavage.

As seen in Figure 4, since the step **5** → **7** has little reverse barrier, the entire process **5** → **7** → **TS(7−8)** should be considered as a single step and gives the highest barrier (without zero-point energy correction); $\Delta E^{\ddagger}$ for the entire isomerization process is 23.7[29.6] kcal/mol. This value is much lower than that for mechanism I and is comparative to the experimental $\Delta H^{\ddagger}$ value of ca. 27 kcal/mol. It is worth pointing out that the small energy difference between **7** and **TS(7−8)** suggests a small activation barrier for the C−C bond cleavage on the tri-Ru complex. This may be due to the multinuclear "cluster effect" in which the adjacent metal cooperates in activating the C−C bond of the ruthenacyclopentadiene ring formed by the other metal center.

Substituted Ruthenacyclopentadienyl Complexes. Although the above calculated energetic barrier for reaction mechanism II is very close to that reported by experiment, one should remember that mono- and dimethyl-substituted complexes are used in the experiment, while calculations are for unsubstituted models. Therefore, here we also investigated the monomethyl- or dimethyl-substituted model complexes **5-α-Me** and **5-α*β*-diMe**. Note that when one uses the monomethyl- or dimethyl-substituted model complexes, **5-α-Me** and **5-α*β*-diMe**, respectively, to explore the isomerization process via mechanism II, there are two possible pathways corresponding to the position of the initial hydride transfer process forming the RuC_4 allyl intermediate **7**. In Figure 5 we present the above-mentioned two pathways, paths II.A and II.B, for the dimethyltriruthenacyclopentadiene complex. Similar pathways, path II.C and path II.D, for the skeletal rearrangement in the monomethyl triruthenacyclopentadiene complex were given in Figure S1 of the Supporting Information and will not be discussed here in detail.

Pathway II.A starts from the initial complex **5-α*β*-diMe**, where methyl groups are located on C^{α} and C^{β} centers and proceeds via transfer of the bridging H1 atom bridged between Ru1 and Ru3 centers to the $C^{\delta}H_2$ group in forming the **7-α*β*-diMe** complex. In the next step, the cleavage of $C^{\gamma}-C^{\delta}$ and formation of $Ru3-C^{\gamma}$ and $Ru3-C^{\delta}$ bonds occur via **TS(7−8)(II.A)**. The resulting complex is the intermediate **8-α*β*-diMe**. Later, the $Ru1-C^{\alpha}$ and $Ru1-C^{\delta}$ bond cleavage and $C^{\alpha}-C^{\delta}$ bond formation take place through **TS(8−7)(II.A)** and lead to formation of the **7-*β*γ-diMe** complex, where the metallacycle already moved from the Ru1 to Ru3 center, and therefore, a new notation of the carbon atoms of the C4 unit (from the Ru3 center) is initiated. In the final step, the **7-*β*γ-diMe** complex rearranges to the final product **5-*ββ*′-diMe** with a small barrier.

Pathway II.B starts from the same initial complex **5-α*β*-diMe** and proceeds via migration of the H2 atom from being bridged between the Ru1 and Ru2 centers to the C^{α} center to form a different isomer of the **7′-α*β*-diMe** complex with the C^{α}HMe group. The resulting complex **7′-α*β*-diMe** rearranges to intermediate **8′-α*β*-diMe** via **TS(7−8)(II.B)**. In complex **8′-α*β*-diMe** the bridging group between the the Ru1 and Ru2 centers

is C^{α}HMe. In the next steps the complex **8′-αβ-diMe** isomerizes to the final product, the **5-αα′-diMe** complex, via transition state **TS(8−7)(II.B)** and intermediate **7-αδ-diMe**. Note that in the last stage of the reaction the notation of the carbon centers of the C4 unit is based on Ru2.

TS(7−8)(II.A), **TS(8−7)(II.A)**, **TS(7−8)(II.B)**, and **TS(8−7)(II.B)** are calculated (based on the single-point energy calculations) to be 26.2[31.5], 20.5[26.1], 51.2-[55.7], and 53.3[57.7] kcal/mol higher than the reactant for **5-αβ-diMe**, respectively. Similar values for the monomethyl triruthenacyclopentadiene complex **5-α-Me** are 23.7[29.6], 23.7[29.6], 54.4[58.9], and 54.5[58.9] kcal/mol at **TS(7−8)(II.C)**, **TS(8−7)(II.C)**, **TS(7−8)(II.D)**, and **TS(8−7)(II.D)**, respectively (see Figure S1 of the Supporting Information and, partially, Figure 4). Thus, in general, the transition states corresponding to path II.A (**TS(7−8)(II.A)** and **TS(8−7)(II.A)** for **5-αβ-diMe**) and path II.C (**TS(7−8)(II.C)** and **TS(8−7)(II.C)** for **5-α-Me**) are ca. 25−30 kcal/mol smaller than those for path B and path D for mono- and di-Me species, respectively, regardless of the basis sets used. Furthermore, the energy barrier for **5-αβ-diMe** at **TS(8−7)-(II.B)** (which corresponds to forward reaction) is about 2 kcal/mol higher than that at **TS(7−8)(II.B)** (which corresponds to reverse reaction). Meanwhile, for path II.A the barrier for forward reaction at **TS(8−7)(II.A)** is about 5−6 kcal/mol smaller than that for reverse reaction at **TS(7−8)(II.A)**. These data suggest that path II.A is more favored over path II.B for **5-αβ-Me.** Similarly, path II.C is more favored over path II.D for **5-α-Me**. This result is consistent with the experimental result, in which only 3,4-dimethyl-substituted product is formed through the reaction. In other words, path II.A is the only route for isomerization of the 2,3-dimethylruthenacyclopentadiene complex.

4. Conclusions

On the basis of the above presented experimental and computational results, one may draw the following conclusions:

Mechanism I, involving the cyclobutadiene species and proceeding via reductive coupling of ruthenacyclopentadiene to form a cyclobutadiene unit followed by C−C bond cleavage of the cyclobutadiene ring, is found to be energetically unfavorable. The calculated rate-determining barrier is ca. 48−55 kcal/mol for both unsubstituted and mono- or/and dimethyl-substituted models.

Multistep hydride-assisted mechanism II, which involves (1) insertion of a C═C double bond into the Ru−H bond, (2) cleavage of a C−C bond to form the allylmethylene complex, (3) reductive coupling to reproduce the RuC4 ring, and (4) C−H bond cleavage to give the final product, is found to be the more favorable one. It proceeds with a 25−30 kcal/mol rate-determining barrier for unsubstituted system, which is comparable with the experimental value of *ca. 27 kcal/mol* reported for mono- and dimethyl-substituted complexes.

Including substituents into calculations increased the calculated rate-determining barrier by only 1−2 kcal/mol. Meanwhile, it made the mechanism more complex. For dimethyl-substituted complexes, **5-αβ-diMe** and **5-γδ-diMe**, we have studied two possible pathways, II.A and II.B, leading to two different products, **5-ββ′-diMe** and **5-αα′-diMe**, respectively. Among these mechanisms, pathway II.A is found to be kinetically more favorable by ca. 25 kcal/mol. Therefore, mechanism II.A leading to formation of 3,4-dimethyl-substituted product is the most favorable mechanism of the isomerization of the 2,3-dimethylruthenacyclopentadiene complex $\{(C_5Me_5)Ru\}_2\{(C_5Me_5)RuCMeCMeCHCH\}(\mu\text{-}H)_3$. This computational finding explains the experimental results that only 3,4-dimethyl product is formed.

Experimental Details

All manipulations were carried out under an argon atmosphere with use of standard Schlenk techniques. Toluene and benzene-d_6 were dried over Na/benzophenone. Cyclopentadiene and methylcyclopentadiene were prepared by depolymerization of the corresponding dimers prior to use. Ruthenacyclopentadiene complexes **1** and **3** were prepared by the reaction of $\{(C_5Me_5)Ru\}_3(\mu\text{-}H)_3(\mu_3\text{-}H)_2$ (**1**) with cyclopentadiene[6a] and methylcyclopentadiene,[6b] respectively.

$\{(C_5Me_5)Ru\}_2\{(C_5Me_5)RuCHCMeCHCH\}(\mu\text{-}H)_3$ (2). 2-Methylruthenacyclopentadiene complex $\{(C_5Me_5)Ru\}_2\{(C_5Me_5)RuCMeCHCHCH\}(\mu\text{-}H)_3$ (**1**) (25.0 mg, 32.1 μmol) was dissolved in 0.5 mL of C_6D_6 in a 5 mm NMR tube and heated at 90 °C for 40 h. By means of ^{1}H NMR spectroscopy, 85% conversion from complex **1** to 3-methylruthenacyclopentadiene complex **2** was confirmed. Removal of the solvent under reduced pressure, followed by recrystallization from THF, gave 9.6 mg of **2** as a dark red crystal (12.3 μmol, 38.3% yield). ^{1}H NMR (400 MHz, 23 °C, C_6D_6): δ 7.10 (d, J = 2.4 Hz, 1 H, RuC*H*−), 7.05 (d, J = 4.5 Hz, 1 H, RuC*H*−), 3.69 (dd, J = 4.5 and 2.4 Hz, 1 H, RuCHC*H*−), 2.02 (s, 3 H, RuCHC*Me*−), 1.84 (s, 15 H, C_5Me_5), 1.82 (s, 15 H, C_5Me_5), 1.78 (s, 15 H, C_5Me_5), −18.38 (brs, 1 H, Ru-*H*), −18.96 (brs, 1 H, Ru-*H*), −20.49 (s, 1 H, Ru-*H*). ^{13}C NMR (100 MHz, 23 °C, C_6D_6): δ 167.9 (s, J_{CH} = 152.6 Hz, Ru*C*H−), 162.0 (d, J_{CH} = 155.0 Hz, Ru*C*H−), 94.6 (s, C_5Me_5), 89.6 (s, C_5Me_5), 88.8 (s, C_5Me_5), 76.8 (s, RuCH*C*Me−), 68.2 (d, J_{CH} = 153.1 Hz, RuCH*C*H−), 24.3 (q, J_{CH} = 122.6 Hz, RuCHC*Me*−), 12.3 (q, J_{CH} = 126.0 Hz, C_5Me_5), 11.7 (q, J_{CH} = 126.1 Hz, C_5Me_5), 11.1 (q, J_{CH} = 126.3 Hz, C_5Me_5). Anal. Calcd for $C_{35}H_{54}Ru_3$: C, 54.03; H, 7.00. Found: C, 53.68; H, 7.34.

$\{(C_5Me_5)Ru\}_2\{(C_5Me_5)RuCHCMeCMeCH\}(\mu\text{-}H)_3$ (4). 2,3-Dimethylruthenacyclopentadiene complex $\{(C_5Me_5)Ru\}_2\{(C_5Me_5)RuCMeCMeCHCH\}(\mu\text{-}H)_3$ (**3**) (75.2 mg, 0.097 mmol) was dissolved in 10 mL of toluene and heated at 110 °C for 18 h. Quantitative conversion of **3** to 3,4-dimethylruthenacyclopentadiene **4** was confirmed by means of ^{1}H NMR spectroscopy. After the solvent was removed under reduced pressure, the resulting brown solid was washed with MeOH. Drying the solid in vacuo afforded the 3,4-dimethylruthenacyclopentadiene complex $\{(C_5Me_5)Ru\}_2\{(C_5Me_5)RuCHCMeCMeCH\}(\mu\text{-}H)_3$ (**4**) as a purple crystalline solid (50.0 mg, 0.064 mmol, 66.5% yield). ^{1}H NMR (300 MHz, 23 °C, C_6D_6): δ 7.13 (s, 2 H, RuC*H*−), 1.84 (s, 6 H, RuCHC*Me*), 1.84 (s, 30 H, C_5Me_5), 1.79 (s, 15 H, C_5Me_5), −18.67 (s, 2 H, Ru-*H*), −20.34 (s, 1 H, Ru-*H*). ^{13}C NMR (125 MHz, 23 °C, C_6D_6): δ 168.5 (d, J_{CH} = 149.3 Hz, Ru*C*H−), 95.0 (s, C_5Me_5), 89.6 (s, C_5Me_5), 77.8 (s, RuCH-*C*Me), 25.6 (q, J_{CH} = 124.1 Hz, RuCHC*Me*−), 13.0 (q, J_{CH} = 124.7 Hz, C_5Me_5), 11.7 (q, J_{CH} = 125.1 Hz, C_5Me_5). Anal. Calcd for $C_{36}H_{56}Ru_3$: C, 54.29; H, 7.13. Found: C, 54.26; H, 6.82.

Kinetics of Thermolysis of *nido*-Ruthenacyclopentadiene Complexes 1−3. Of all samples, *nido*-2-methylruthenacyclopentadiene complex **1** was weighed out in a 5 mm NMR tube and 0.5 mL of C_6D_6 was added. The reaction proceeded at 85, 100, 115, 130, and 145 °C. The consumption of **1** was monitored at each temperature by ^{1}H NMR, and the resonance at δ −21.76 and −20.49 were integrated periodically. These correspond to hydride resonances for **1**. At regular

time intervals, the percentage of **1** was calculated by dividing the integral value for **1** by the sum of the integral values for complexes **1** and **2**. This value was used for the determination of the rate constant. Temperature dependence of the rate constant was used in deriving activation parameters, $\Delta H^{\ddagger}$ and $\Delta S^{\ddagger}$. Kinetics experiments for thermolysis of **3** were carried out by the same procedure mentioned above. The reaction proceeded at 70 , 85, 100, 115, and 130 °C.

X-ray Structure Determination of 2. Crystals suitable for a diffraction study were grown from THF. Mo Kα radiation was used ($\lambda = 0.71069$ Å), and the structures were solved and expanded using Fourier techniques.[21] Due to the disordered structure, C1, C2, C3, C4, and C5 are refined isotropically while the rest were refined anisotropically. Ruthenacyclopentadiene carbons C2/C2A and C4/C4A are disordered with thermal parameters of 50% occupancy, respectively. H atoms were included but not refined. Other details of data collection and refinement are given in the Supporting Information.

(21) DIRDIF92: Beurskens, P. T.; Admiraal, G.; Beurskens, G.; Bosman, W. P.; Garcia-Granda, S.; Gould, R. O.; Smits, J. M. M.; Smykalla, C. The DIRDIF program system; Technical Report of the Crystallography Laboratory; University of Nijmegen: The Netherlands, 1992.

Acknowledgment. The authors are grateful to Dr. Dmitry V. Khoroshun and Dr. Masato Oshima for valuable discussions. A.I. acknowledges the Postdoctoral Fellowship from the Japan Society for Promotion of Science. The present research is in part supported by a grant (CHE-9627775 and CHE-0209660) from the National Science Foundation. Acknowledgment is made to the Cherry L. Emerson Center of Emory University for the use of its resources, which is in part supported by a National Science Foundation grant (CHE-0079627) and an IBM Shared University Research Award.

Supporting Information Available: Tables of Cartesian coordinates and total energies of all the optimized structures and the experimental procedures for the kinetic studies, obtained kinetic parameters, and spectral data for complex **2** and **4**. In Figure S1 we have presented two possible pathways, path II.C and path II.D, for the skeletal rearrangement in the monomethyl triruthenacyclopentadiene complex. This material is available free of charge via the Internet at http://pubs.acs.org.

OM030046B